Food Research International 164 (2023) 112394

Contents lists available at ScienceDirect

Food Research International

journal homepage: www.elsevier.com/locate/foodres

Wakame replacement alters the metabolic profile of wheat noodles after *in vitro* digestion

Yi Kai [a], Yi Liu [a,b], Hongliang Li [c], Hongshun Yang [a,b,*]

[a] Department of Food Science and Technology, National University of Singapore, Singapore 117542, Singapore
[b] National University of Singapore (Suzhou) Research Institute, 377 Lin Quan Street, Suzhou Industrial Park, Suzhou, Jiangsu 215123, PR China
[c] Guangzhou Welbon Biological Technology Co., Ltd, Guangzhou, Guangdong 523660, PR China

ARTICLE INFO

Keywords:
Seaweed
Food metabolomics
Nuclear magnetic resonance
Rheology
Microstructure
Noodle
Metabolite

ABSTRACT

The development of nutritional noodles of high quality has become a new hotspot of research in the area of food science. Since wakame is edible seaweed rich in dietary fiber and proteins and rarely found in ordinary noodle, this study investigated the release of metabolites, the texture quality, and the rheological properties of wakame noodle, as well as the mechanism by which extruded wakame flours can influence noodle texture and viscoelasticity through digestion. Basically, nuclear magnetic resonance spectra were applied to identify the 46 metabolites including amino acids, saccharides, fatty acids, and other metabolites. Both PCA and OPLS-DA model showed fit goodness and good predictivity, which were assessed the increasing release of most metabolites. Structural studies discussed the effects on the enhancement of interlinkage with gluten matrix and protein matrix, which were validated via the decreasing instantaneous compliance J_0 (1.64×10^{-5} to 0.16×10^{-5} Pa^{-1}). Wakame addition best matched the physiochemical properties of noodle, in terms of chewiness (99.10 vs 122.66 g.mm), gumminess (281.98 vs. 323.44 g), and gel strength (132.65 vs 173.95 kPa•s^{-1}). Beyond the functional characteristics it contributes benefits like reduction of diet-related diabetes. As a consequence, the creation of personalized nutritious, healthy noodles will be an innovative route from a scientific viewpoint and an application standpoint.

1. Introduction

While refined flour still dominates the noodles ingredient market (Zhu, Liu, Chen & Zheng, 2022), changing consumer eating habits and sustainability concerns are causing innovate noodles to emerge as a new trend (Ribeiro et al., 2022). Moreover, due to the insufficient nutritional function of traditional noodles ingredient including wheat flour, there has been a new focus on seaweed as a high-fiber food source, as well as providing consumers with proteins, bioactive compounds, minerals, and vitamins (Rawiwan, Peng, Paramayuda, & Quek, 2022).

The main catalogues of seaweeds are as follows: green (*chlorophytes*), red (*rhodophytes*), and brown (*phaeophytes*), in which several bioactive compounds are found in brown seaweed (e.g., fucosterol, polyphenols, omega-3 polyunsaturated fatty acids, et al.) as mentioned in previous epidemiological studies (Fitzgerald et al., 2012). Moreover, brown seaweed has for centuries been a traditional food in Asian diets, while in the western world, predominantly as functional pharmaceutical or food ingredients. According to studies of *Undaria pinnatifida*, it contains 15–24% of protein, which is higher than most brown seaweeds, which contain 15% (Nadeeshani, Hassouna, & Lu, 2021; Rioux, Beaulieu, & Turgeon, 2017).

It was also named as wakame, which is the processed *Undaria pinnatifida* as food ingredients inhibiting high productivity due to the implemented policy that allowed farming and harvesting of *Undaria pinnatifida* in late 2020 (Cho, Kim, & Kim, 2013; Fung, Hamid, & Lu, 2013; Kim, Ra, & Kim, 2013). Growing rate for the productivity of wakame is high and paving the way for the expansion of wakame in western diets is a growing trend but still very challenging (Roberts, Paul,

Abbreviations: **WKN 5**, wakame noodles at 5% wakame powder replacement; **WKN 10**, wakame noodles at 10% wakame powder replacement; **WKN 15**, wakame noodles at 15% wakame powder replacement; **WKN 20**, wakame noodles at 20% wakame powder replacement; **NMR**, Nuclear magnetic resonance; **PCA**, The principal component analysis; **OPLS-DA**, Orthogonal projection to latent structures-discriminant analysis; **FTIR**, Fourier-transform infrared spectroscopy; **SEM**, Scanning electron microscope.

* Corresponding author at: Department of Food Science and Technology, National University of Singapore, Singapore 117542, Singapore.
E-mail address: fstynghs@nus.edu.sg (H. Yang).

https://doi.org/10.1016/j.foodres.2022.112394
Received 4 October 2022; Received in revised form 14 December 2022; Accepted 24 December 2022
Available online 28 December 2022

Dworjanyn, Bird, & de Nys, 2015). Regarding this issue, the recommended approach is an option for dietary intake that meets an adequate nutritional requirement without changing consumers' eating habits. As a result, substantial effort should be expended both on overcoming the technological obstacles and on optimizing combination of food and wakame. In addition, the inclusion of wakame flour with high concentration in noodles has not yet been extensively explored.

The objective of this report was to develop an improved noodle product containing a higher level of nutritional function. This study evaluated the effects of wakame on the *in-vitro* digestive performance through nuclear magnetic resonance (NMR) spectroscopy, chemical structural changes, noodle surface morphology, and physical-chemical properties, such as rheology and texture profiles. In addition, NMR prevents the effect of overestimating the protein content of wakame noodle (WKN), for example by identifying nucleic acids as well as non-protein nitrogen sources as "proteins". Overall, this metabolic analysis has been performed preliminarily *in vitro*, which is a promising method to estimate the nutritional quality of wakame noodles, particularly for protein and other components (Lucas-Gonzalez, Viuda-Martos, Perez-Alvarez, & Fernandez-Lopez, 2018).

2. Materials and methods

2.1. Materials

Common wakame (*Undaria pinnatififida*) was purchased at a food processing manufacturer under the brand name "Nature Glory" (Singapore), which was harvested in clean seas of Japan, they scanned every batch for radiation with in-house Geiger equipment. Crushed seaweed was passed through an 80-mesh sieve. The major nutritional proximate characteristics of wakame were obtained by the manufacturer as following, the water, protein, fat, carbohydrate, fiber, and ash of wakame were 13.0%, 15.0%, 3.2%, 35.3%, 2.7% and 30.8%, separately. The wheat flour was replaced by wakame flour as different level of mixtures which were used in this study. Salt and wheat flour with no additives added were provided by a local supermarket in Singapore. Purified deionised water (DI water) used was with system (Millipore, Billerica, MA, USA). All other chemicals and reagents used were of analytical grade.

2.2. Wakame dough and noodle processing

At the setting of a total flour weight of 150 g, the wakame flour at the 0% (0 g), 5% (7.5 g), 10% (15 g), 15% (22.5 g), 20% (30 g) of total weight was mixed to replace the wheat flour and then processed into noodles. Different contents of wakame flour and the corresponding wheat flour (total weight of both flours is constant 150 g) was mixed with suitable amount of deionised water (DI water). The water content, resting time and best boiling time were determined by the previous study with slight modification (Xu, Hou, Ding, & Du, 2020). According to the preliminary testing, when the content of additives excesses 15%, the quality begins to show a decreasing trend, and the sensory evaluation of the noodles has a crumbly feeling. In this way, 20% was set as the maximum concentration. Then put them into a self-sealing bag in 30 min for dough resting.

The dough was calendared at 4.8 mm roll spacing and folded at thinner roll 5 times to 2 mm thick, respectively. This was done for enable insertion into the cutting roll before cutting dough into 150 mm wide noodles. Then noodle with consistent appearance and length was placed in a stainless-steel basin for 30 min to dry it for subsequent experiments.

Twenty units of raw noodles were put into 15 times the mass of noodles in boiling water with 2000 W power induction oven until the optimal cooking time, which is set to 6 min depending on the disappear of white core inside the noodles. Boiling the noodles for 30 s, then cooling them in cold water for 30 s and quickly put on filter paper to absorb the water. The samples were used for analysis to determine the textural properties of the noodles after cooking.

2.3. Texture analysis and cooking properties of wakame noodle

The texture of raw dough was evaluated by a TA.XT2i Texture Analyzer (Stable Micro Systems Co. Ltd., Godalming, UK) based on Xu et al. (2022). The raw dough samples were cut into cubes of 25 mm and then compressed using a cylindrical probe with the diameter of 25 mm. The test strain rate, speed, compression trigger force and interval time were 70%, 0.8 mm/s, 20 g and 1 s, respectively. Within 15 min of cooking, five textural parameters (hardness, cohesiveness, springiness, chewiness, and resilience) were assessed.

Water absorption and cooking loss of the wakame-added noodles were determined according to Zhang, Zhang, Li, and Sun (2021) with minor modifications. Briefly, noodle strands (20 g) were cooked in 450 mL of boiling water to optimum cooking time of each noodle sample. Afterwards, cooked noodles were immediately rinsed with distilled water for 1 min, subsequently drained for 5 min, and weighed. Water absorption was defined as the ration of water the noodles absorb during cooking to their initial weight.

Cooking loss of the wakame-added noodles were characterized by measuring the turbidity of the cooled noodle soup at 675 nm using a microplate reader (BioTek Synergy HTX, Agilent Technologies, Inc., United States).

2.4. Color changes

Color analysis for noodle samples was conducted according to Zhou, Liu, Kang, Cui, and Yang (2021). A colorimeter (CM-3500d, Konica Minolta, Inc., Japan) was used to measure the L^*, a^* and b^* of cooked noodles. Following is the formula for calculating *whiteness*:

$$Whiteness = 100 - \sqrt{(100 - L*)^2 + a*^2 + b*^2} \quad (1)$$

where L^* presents lightness; a^* presents redness/greenness; b^* presents yellowness/blueness. The analysis was repeated nine times for each group.

2.5. In-vitro digestion

WKW noodle digestra were prepared according to the method of Ran, Yang, Chen, and Yang (2022). The three steps during digestion were carried out according to the previously described references (Fabek, Messerschmidt, Brulport, & Goff, 2014) to mimic oral, gastric, and small intestinal digestion, which built a standardised static *in vitro* digestion model that has been used widely in different food studies.

For oral digestion, the MSF (mimicked salivary fluid) was prepared as described by Ran and others (2022). Briefly, 150 mg of α-amylase was added to a glass bottle containing 5 g of sample and MSF. A final pH of 7 was adjusted by HCl within 5.0 mL of MSF (1.5% HCl (w/w) in 2.5% $CaCl_2$ (w/w)). In a water bath, the mixture was dissolved and heated for 5 min with stirring at 200 rpm.

For gastric digestion, the MGF (mimicked gastric fluid) has been prepared as described above mentioned. Briefly, 19.15 mg of pepsin was added to a glass bottle containing 5 g of sample and MGF. A final pH of 3 was adjusted by HCl within 5.0 mL of MGF (0.025% $CaCl_2$ (w/w) in 50% HCl (w/w)). In a water bath, the mixture was dissolved and heated for 5 min with stirring at 200 rpm.

For intestinal digestion, the MIF (mimicked intestinal fluid) has been prepared as described above mentioned. Briefly, 200 mg pancreatin was added to a glass bottle containing 5 g of sample and MIF. A final pH of 7 was adjusted by HCl within 5.0 mL MIF [$CaCl_2$ (10%, w/w) in 10% NaOH (w/w)]. In a water bath, the mixture was dissolved and heated for 5 min with stirring at 200 rpm.

The digesta were then placed in the boiling water immediately for 10 min to terminate the activity of digestive enzymes and then cooled down

at room temperature with ice. Moreover, the digesta were stored at −70 ℃ overnight and further frozen in freeze-drying for the following test.

2.6. NMR spectroscopy

For NMR measurement, the metabolites procedure was carried out with some modifications as described by Huang, Zhao, Mao, Chen, & Yang (2021).

At first, the trichloroacetic acid (TCA) extraction was prepared. Following centrifugation (12000 *g*, 4 °C, 10 min), the obtained supernatants were filtered using microporous membranes of 0.22 μm.

Then, the 50 mg of freeze-dried WK digesta of five concentration groups prepared in Section 2.5. was mixed with 2 mL D_2O (deuterated water) with 1 mM of 3-trimethylsilyl [2,2,3,3-d4] propionate (TSP, Sigma-Aldrich, St Louis, MO, USA) as internal chemical shift reference, respectively and centrifuged at 12,000 *g* at 4 ℃ (10 min). After that, the 550 μL supernatant after filtration via 0.22 μm microporous membrane was conducted in triplicate for NMR test.

With a triple inverse gradient probe applied to a 500.23 MHz frequency Bruker NMR spectrometer (DRX-500, Bruker, Rheinstetten, Germany), all NMR measurements were conducted. All the data were obtained by 128 scans and a 2 s of relaxation delay. For selected samples, the 2D $^{1}H–^{13}C$ NMR spectra were applied by heteronuclear single quantum correlation (HSQC), and the ^{13}C spectrum was acquired with a range of 180 ppm.

The baseline and phase correction of NMR spectra of five concentration groups were performed by the software Topspin 4.1.4 (Bruker) and MestReNova 12.0.3 (Mestrelab Research, S.L., Spain). Afterward, the range of TSP resonance (-0.01 to 0.01 ppm) was normalized and then integrated. Moreover, the 2D $^{1}H–^{13}C$ and 1D ^{1}H spectrums were then analyzed for the metabolites identification according to the Human Metabolome Database (https://hmdb.ca/) and Biological Magnetic Resonance Data Bank (http://www.bmrb.wisc.edu/metabolomics/).

For group separation and pairwise comparison, Principal Component Analysis (PCA) and Orthogonal Projection to Latent Structures-Discriminant Analysis (OPLS-DA) were used, respectively, using SIMCA software (version 13.0; Umetrics, Umeå, Sweden). The selection standard (projection VIP > 1, P value < 0.05) was used to determine the statistically significant metabolites. The pathway analysis was performed by MetaboAnalyst 5.0 (https://www.metaboanalyst.ca/) to diagnose the significant pathways.

2.7. Confocal laser scanning microscopy (CLSM)

The CLSM imaged samples were prepared according to a pervious study with slight modifications (Ma et al., 2022). Digesta sample (20 mg) were dispersed in 1 mL of the mixture of Nile red and FITC dyes at a ratio of 0.1% (w/v). Samples labelled by fluoresceine in ethanol were rest at room temperature for 0.5 h, then centrifuged and washed ten times with ethanol until the supernatant is clear. A Zeiss LSM710 confocal laser scanning microscope (Carl Zeiss Inc., Braunschweig, Germany) equipped with argon-ion and helium-neon (He-Ne) lasers 488/643 was utilized for CLSM imaging. These excitations were selected by the range of light wavelengths that add energy to the FITC and Nile Red, respectively. A glass slide was coated with fluorescently labelled solid samples and photographed under a 10× magnification (PlanApo 60×/1.0 WLSM 0.17). For each sample, 10 images were processed using the microscopic imaging software Zen (Jena, German).

2.8. Apparent viscosity and viscoelasticity and rheological modelling

A 25 mm diameter parallel plate of MCR-102 rheometer (Anton Paar, Austria) was used to analyze the rheological properties of the WKN and digesta. The digesta samples were deposited on to the sample holder with the 1.0 mm of distance from holder to the plate for 3 min as temperature equilibrium requisite. For the strain sweep measurements, each sample was measured at 0.1% strain to attain the linear viscoelastic region. Tests were conducted between 0.1 and 100 rad/s for the frequency sweep, and the storage modulus (G′) and loss modulus (G″) were measured. For the shear rate, tests were managed from 0.01 to 20 s^{-1}. For the creep recovery, 100 Pa constant shear stress was used from 0 to 373.5 s. Each sample was recorded at least three times every measurement.

Based on the power-law function, the angular frequency (ω), and complex viscosity (η*) was applied as follows:

$$\eta^{*} = K_f \bullet \omega^{n} \tag{2}$$

where K_f represents the intercepts and n represents the slopes indicating the correlation in the gel network, which ranges from 0 (the viscous state) to 1 (elastic state).

Based on the Burgers model, the effects of creep time on instantaneous elasticity, retarded elasticity, and viscous deformation are further investigated as follows:

For creep phase:

$$J_1(t) = J_0 + \sum\left(J_i \bullet \left(1 - exp\left(\frac{-t}{r_i}\right)\right)\right) + \frac{t}{\mu_0}, i = 1,2,3 \tag{3}$$

where $J_1(t)$ represents the creep compliance equation, J_0 is the instantaneous compliance, J_i is the retarded elastic compliances, r_i is the retardation times and μ_0 is the steady state viscosity, which represents the zero-shear viscosity of samples.

For recovery phase:

$$J_2(t) = J_0 + \sum\left(J_i \bullet \left(1 - exp\left(\frac{-t}{r_i}\right)\right)\right), i = 1,2,3 \tag{4}$$

where $J_2(t)$ represents the recovery compliance equation, J_0 is the elastic strain, J_i is the modulus of elasticity of relaxation response, r_i is the retardation times.

The goodness-of-fit was expressed as R^2, RMSE (Root Mean Squared Error), and SSE (Sum of Squares Error), which were determined as follows:

$$RMSE = \sqrt{\frac{\sum(residual^2)}{n-1}} \tag{5}$$

$$SSE = residual^2 \tag{6}$$

where *n* is n is the number of values in total, *residual* is the distance of a point from a curve.

2.9. Scanning electron microscopy (SEM)

SEM images of lyophilized noodle samples were observed using a scanning electron microscope (JEOL JSM-6701F, Tokyo, Japan) at an accelerating voltage of 3.0 kV.

2.10. FTIR

Chemical structures of cooked noodle samples were investigated using a Spectrum One FTIR spectrometer (PerkinElmer, Waltham, MA, U.S.A.) with wavelength range of 4000–450 cm^{-1} at 4 cm^{-1} resolution and 32 scans. Fourier self-deconvolution was performed at the amide I region (1700–1600 cm^{-1}) using the Omnic software 8.2 (Thermo Fisher Scientific Inc. Waltham, MA, U.S.A) with the settings of 30 cm^{-1} bandwidth and 1.3 enhancement factor, followed by curve normalization.

2.11. Statistical analysis

IBM SPSS Statistics 25 was used for the analysis of the data.The

Table 1
Physiochemical properties of boiled noodles prepared with different amount of wakame powder at 0%, 5%, 10%, 15%, 20%.

	0%	5%	10%	15%	20%
LAB					
L^*	63.88 ± 0.18^{a}	51.46 ± 0.37^{b}	41.75 ± 0.57^{c}	36.83 ± 0.47^{d}	33.13 ± 0.25^{e}
a^*	1.24 ± 0.01^{a}	0.52 ± 0.01^{c}	0.56 ± 0.01^{b}	0.33 ± 0.02^{d}	0.03 ± 0.01^{e}
b^*	17.21 ± 0.03^{c}	19.63 ± 0.01^{a}	18.19 ± 0.19^{b}	14.76 ± 0.44^{d}	12.25 ± 0.26^{e}
Whiteness	59.97 ± 0.01^{a}	47.64 ± 0.03^{b}	38.97 ± 0.05^{c}	35.13 ± 0.05^{d}	32.02 ± 0.02^{e}
Textural properties					
Hardness	202.34 ± 25.64^{e}	381.59 ± 22.51^{d}	553.17 ± 31.41^{c}	768.13 ± 15.44^{b}	1198.94 ± 117.68^{a}
Cohesiveness	0.41 ± 0.00^{c}	0.45 ± 0.01^{b}	0.48 ± 0.00^{a}	0.42 ± 0.00^{c}	0.42 ± 0.02^{c}
Springiness	0.38 ± 0.01^{b}	0.36 ± 0.01^{bc}	0.38 ± 0.01^{b}	0.34 ± 0.01^{c}	0.32 ± 0.00^{d}
Gumminess	118.10 ± 18.74^{d}	234.74 ± 12.12^{c}	293.60 ± 2.71^{b}	312.86 ± 8.81^{b}	389.10 ± 16.93^{a}
Chewiness	35.82 ± 5.61^{d}	87.94 ± 4.97^{c}	111.80 ± 2.39^{b}	104.02 ± 4.28^{b}	137.12 ± 12.78^{a}
Resilience	0.10 ± 0.00^{e}	0.11 ± 0.00^{d}	0.14 ± 0.00^{a}	0.12 ± 0.00^{c}	0.12 ± 0.00^{b}

Different superscript letters in rows are significantly different using one-way ANOVA and Duncan's multiple range test ($P < 0.05$). Each point corresponds to the average value ± standard deviation.

reported variables are listed as means ± standard deviation (SD) with three replicates. One-way analysis of variance (ANOVA) was conducted followed by descriptive statistics and Waller-Duncan tests to evaluate the difference between samples with five levels of wakame contents. The differences in means were considered significantly different at $P < 0.05$.

3. Results and discussions

3.1. Effects of wakame addition on the color of wakame noodles

The whiteness of production is the most popular indicator when evaluating the color quality of food production. Table 1 shows the results of color characteristics of control and WKN before and after heat treatment. The L^*, a^* and b^* values decreased with the increasing concentrations of wakame in the designed formulations compared to the wheat flour added. In the current research, the decrease of the whiteness of raw dough may be due to the increasing amount of dietary fibers, sodium alginate and other colored pigments that present in the wakame, as well as the composition of protein upon the dough producing process (Nawaz, et al., 2018). Incorporation of different proportion of the reducing sugar and protein increased the absorption of blue and green light (Gasparre & Rosell, 2019; Mudgil, Barak, & Khatkar, 2016). This might donate the decreasing trend of greenness (a^*) and blueness (b^*) values, thus the samples became darker as shown in the Table 1. The lowest whiteness value was obtained by the WKN 20, thus, the addition of wakame within limits is acceptable but an excessive amount can be visually unappealing.

3.2. Texture profile analysis and cooking properties of wakame noodle

Table 1 shows texture properties of wakame noodles. The cohesiveness is closely associated with gluten, which are bound by the strong internal chemical linkage (Guo, Wei, & Zhu, 2017). The springiness can be considered as an indicator of the energy required for recovery after compression, and the chewiness and gumminess may indicate the energy needed for swallowing-ready state of noodles (Mudgil, et al., 2016). The cohesiveness, springiness, and resilience were slightly increased while the adhesiveness and gumminess of WKN showed a dramatical increase compared to the control group. This result could be due to more gluten which combined by disulfide bonds between glutenin, and gliadin may exit in WKN after cooking (Liu, et al., 2018). The increase of hardness could be attributed to a tight protein network (Guo, Wei, & Zhu, 2017). Corresponding to the further structural properties in our study, nearly all cysteine residues linked to glutamines may serve as donators of the helical structures of glutenin (Khatkar, Barak, & Mudgil, 2013), which also suggested the formation of the viscoelastic gluten network (Khatkar, et al., 2013). There is also a significant impact of hydrogen bonds on the secondary structure and viscoelasticity (Khatkar, et al., 2013). The addition of wakame strengthens the gluten network in the noodles, increasing their cohesiveness and disulfide bonding (Cao, et al., 2021). Consequently, increase in the concentration of wakame (5% to 20% addition) improved the multidimensional texture quality of the wakame noodles quantitatively with good reproducibility (Li, Dhital, & Wei, 2017).

Water absorption is an important indicator that reflects the degree of starch granules absorbing water and swelling during cooking process, which is one of the determinants to noodle quality (Shao, Guo, Li, & Zhu, 2019). As shown in Fig. 11F, wakame showed a great impact on water absorption of wheat-based noodles that with increasing content of wakame in noodle samples, significant decrease in water absorption was observed from 94.37% (control) to 68.83% (15% of wakame addition). Reduction of water absorption could be ascribed to the presence of dietary fibre that might entrap starch granules from absorbing water during cooking process. Interestingly, water absorption of noodles with 20% of wakame replacement rebounds to 73.65% as compared to its counterpart (15% of wakame addition), which might result from the dilution effect of wakame on gluten content in noodles that weakens the protein cross-linking network, thereby facilitating the water penetration from outside (Ojukwu, Tan, & Easa, 2020).

Cooking loss is traditionally used to evaluate the noodle structural integrity during cooking process, which can be characterized by measurement of cooking water turbidity of noodle soup (Zhang et al., 2021). In our study, wheat-based noodles (control) exhibited the lowest cooking loss, with absorbance of 0.153 (Fig. 11G). Replacement of wheat starch with wakame significantly increased the absorbance of the soups of the cooked noodle samples to 0.577 when 20% of wakame incorporated, as a result of the leaching of soluble solids from deterioration of gluten network, which might be explained by that wakame addition dilutes the proportion of wheat gluten proteins in noodles, especially those with 15% and 20% of wakame incorporation, thus further weakens the gluten structure (Fig. 11A-E). Although addition of 5% and 10% wakame results in slightly opaque noodle soup as compared to the control, the soup turbidity is still acceptable when consumed.

3.3. Overview of metabolites profiles in wakame and wheat noodle

The ^{1}H NMR spectra of five concentration levels of wakame noodle after *in-vitro* digestion are shown in Fig. 1. They showed a similar overall chemical shift range which was an indication of close individual metabolites among increasing concentration of wakame addition to the wheat flour noodle. Taken WKN20 as an example, amino acids and carbohydrates were characterized by chemical shifts clustered between 0 ppm and 5 ppm agreeing to previous research (Chen, et al., 2022). The chemical shifts located at 5–10 ppm were also recorded as typical polysaccharides and fatty acids, which were previously detected in spectra. One-to-one referring to the 2D ^{1}H–^{13}C spectra file, verification of the identity of around 46 metabolites has been summarized and shown in Table S1.

In Wakame noodle, 46 compounds including amino acids (e.g., Alanine, Lysine), fatty acids (e.g., Linoleic acid), organic acids (e.g., Succinate), sugars (e.g., Xylitol) and other metabolites (e.g., Betaine) were detected. The results were in accordance with the amino acid profile of proteins from seaweeds (Rawiwan, et al., 2022) and the

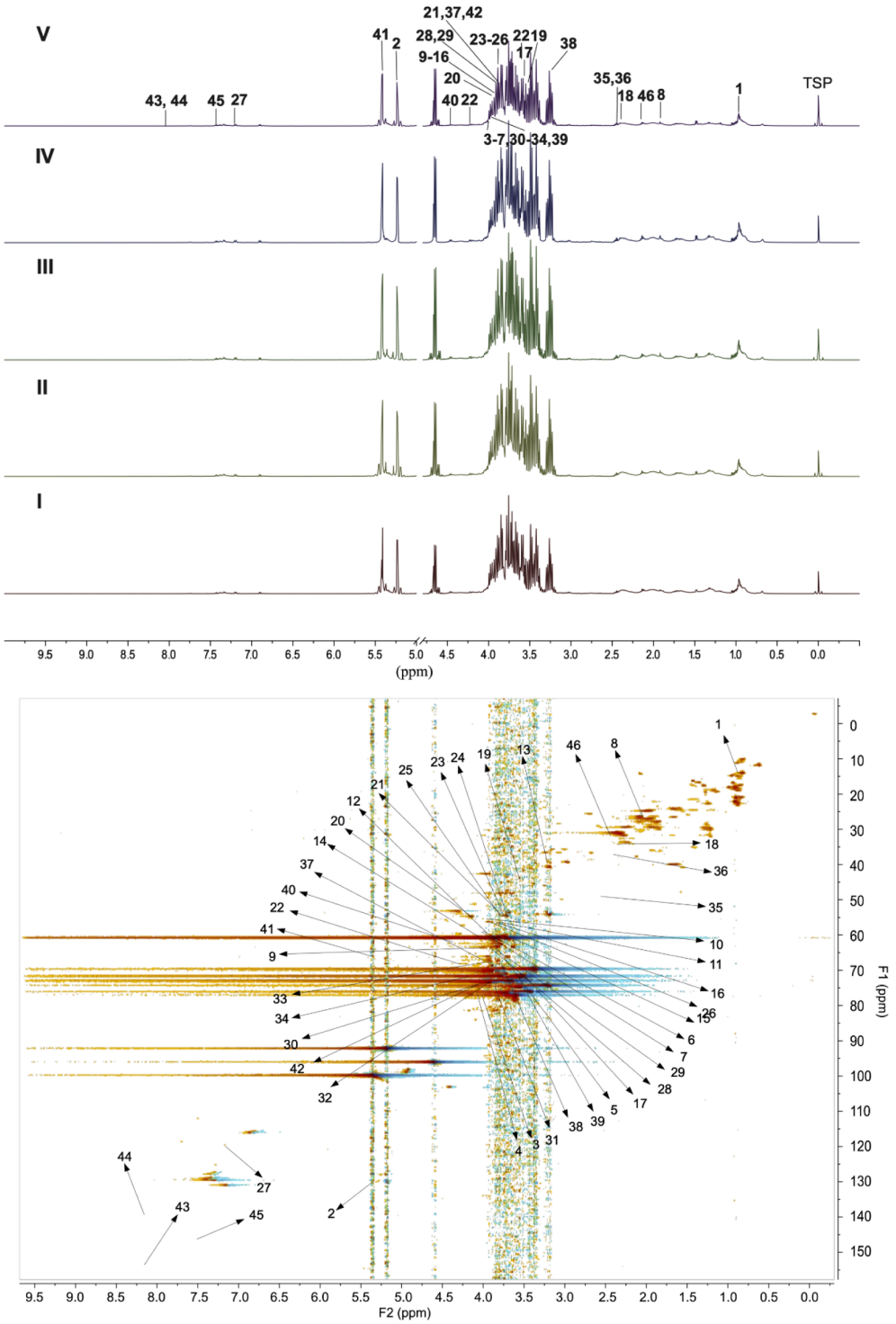

Fig. 1. The NMR ^{1}H and 2D spectra of the wakame noodle (WKN) and wheat-flour noodle after digestion. Note: group II-V represent WKN5, WKN10, WKN15, and WKN20, respectively. Note: WKN 5, WKN 10, WKN 15 and WKN20 represents noodle at 5%, 10%, 15% and 20% wakame powder replacement, respectively.

metabolites of sponge cake after *in vitro* digestion (Huang, et al., 2021).

3.4. Metabolic changes of in vitro digesta of wakame noodle

Fig. 2A illustrates the parameters of the model quality that were determined through principal component analysis (PCA) of metabolite differences. $R^2X = 0.936$ and $Q^2 = 0.878$ showed that the model could well fit and predict the variable. The five groups were separated into five clusters on scores plotting (Fig. 2C). The PCA loading plot enabled the observation of weighted average of the metabolites with weights PC1 in the first dimension and PC2 in the second dimension among different treatments. As shown in loading plot Fig. 2C, metabolites such as histidine, 5-oxoproline, linoleic acid, methionine, fructose, and valine had a higher loading in PC1 while there was a greater contribution of adenine, hypoxanthine, and tyrosine in PC2. Those metabolites might be indicated as significant biomarkers which existed in different concentrations.

The spectra of the control and WKN10 group (Fig. 3), control and

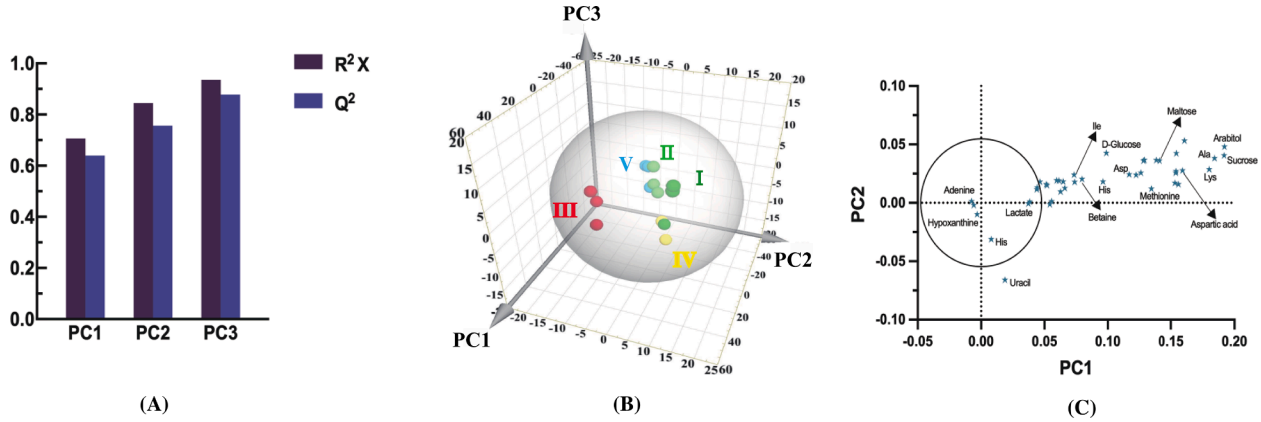

Fig. 2. The principal component analysis (PCA) for wakame noodle and wheat-based noodle. (A) Fitting summary for PCA model; (B) The 3D scores plotting of PCA; (C) The loading plotting of PCA. Note: group I, II, III, IV, and V represent control group, WKN5, WKN10, WKN15, and WKN20, respectively. Note: WKN 5, WKN 10, WKN 15 and WKN20 represents noodle at 5%, 10%, 15% and 20% wakame powder replacement, respectively.

WKN15 group (Fig. 3), control and WKN20 group (Fig. 3) were also analyzed synergistically using OPLS-DA to parallelly detect changes in metabolites with different concentrations. As shown in Fig. 3 left, orthogonally score plots showed the possible presence of similarities between groups as well as Fig. 3 right showed the parallel coefficient plots. All these three OPLS-DA models indicated good predictability and fitness ($R^2X = 0.94$, $Q^2 = 0.88$) because both R^2 and Q^2 were > 0.8. Moreover, each pair was far away from each other that indicated strong metabolic difference was generated with and without wakame addition (Fig. 3 right).

The values of coefficient plotted (Fig. 3 left) derived from ^{1}H NMR binned data and the blocks above the axis suggested higher than control group, whereas others below the axis suggested metabolites that are higher at the control group, among which 5 metabolites (e.g., palmitic acid, allantoin, oleic acid, methionine, and fructose) showed notably increased relative contents in the WKN 10 sample than control sample. For WKN 15 sample, some metabolites such as oleic acid, inositol and asparagine showed opposite tendency compared with it in WKN 10 group, and other products that were also identified as key metabolites remained on the same trend. Furthermore, though eight metabolites of WKN 15 digesta were suggested higher than control that showed the increase over the WKN 10 group, more than half of total metabolites were still lower without wakame addition.

After 15% wakame addition, several amino acids were observed to increase compared to the control (e.g., methionine and histidine), and histidine which was also observed to increase as compared to the WKN 10. However, the WKN 20 sample presented a higher amino acid content than control and only 4 metabolites decreased, including lactate, lysine, methionine, and histidine. This observation has been proved via previous research, which concluded that the presence of protein from wakame partially countered the decrease of the protein digestibility of noodles (Opazo-Navarrete, Tagle Freire, Boom, & Janssen, 2018).

To further understand the difference in metabolite release, the coefficient results as well as VIP score (Table S2-S4) were also applied to recognize significant metabolites after *in vitro* digestion based on VIP > 1 and $P < 0.05$ (Zhao, Chen, Wu, He, & Yang, 2020), such as uracil, D-proline, alanine, sucrose, lactate, aspartic acid, glycerophosphate and so forth were shown as a result of model I (WKN10). Generally, forty metabolites contributed to the weight of model I (WKN 10) compared to thirty-eight metabolites were selected based on the VIP scores and coefficient value of model III (WKN 20), suggesting that wakame would inhibit the metabolite release after *in vitro* digestion due to the wakame addition level, which was understandable with the different fiber content between wakame and starch. This observation would be further proved and explained in Section 3.10.

Moreover, as shown in the coefficient value of control group compared to WKN 20 group, most metabolites such as uracil, palmitic acid, phenylalanine, leucine, linoleic acid, glutamine, sucrose, lysine, isoleucine and so forth were elevated, suggesting that higher wakame concentration contribute to more metabolic contents. This observation would be further illustrated in Section 3.9.

3.5. Heat map metabolite profiles in wakame and wheat flour noodle

The horizontal view of heatmap was mainly plotted on a blue-red view and visually characterized by the statistically significant metabolite concentrations in various noodles with different concentrations of wakame flour addition after *in vitro* digestion. Fifty-five metabolites were simultaneously identified, among which sucrose, alanine and arabitol were drastically increased after wakame addition, as shown in red blocks, (Fig. 4) compared to other metabolites such as aspartic acid, glycerophosphorylcholine, lysine, mannitol, and fructose, which increased faintly. In contrast, some metabolites (adenine, hypoxanthine, uracil, histidine, and lactate etc.), presented in a spectrum of bluish colors, were decreased harshly compared to other metabolites (choline, tryptophan, D-Glucose, phenylalanine, and asparagine etc.) which showed slightly decrease.

Furthermore, 16 amino acids were identified which represented the most dominant category in all samples compared to 8 sugars, 6 organic acids and 8 other metabolites which were depleted. In another study (Rafiquzzaman, et al., 2015; L. Wang, Park, Jeon, & Ryu, 2018), it stated that the molecular weight and structural characteristics of peptides determine the movement and penetration of peptides during digestion. In this way, peptides and protein hydrolysate from wakame are presumably to incorporate free radical scavenging activities. Hence, WKN may help for the prevention of diseases caused by inflammatory or oxidative-stress due to a good antioxidant potential (Kang, Kim, Kwon, & Ha, 2008). Therefore, this heatmap revealed that incorporation of wakame not only raised amino acid pattern of noodles but also improved the antioxidant activities.

3.6. Alternation of metabolic pathways of wakame noodle

To further investigate the difference in the glucose release and NMR tests of the wakame addition noodles compared to the control group, we explored the pathway by MetaboAnalyst 5.0. to evaluate the interference in each group's metabolic networks with and without wakame addition based on the significant metabolites identified in 3.2 (recorded in Table. S5 and circled in Fig. 5). Based on $-\log_{10}(P) > 1.301$, the significant pathways were summarized in Table S5. Totally, forty-six pathways were involved and thirteen of metabolic pathways were significantly affected on the WKN 10 sample through *in vitro* digestion,

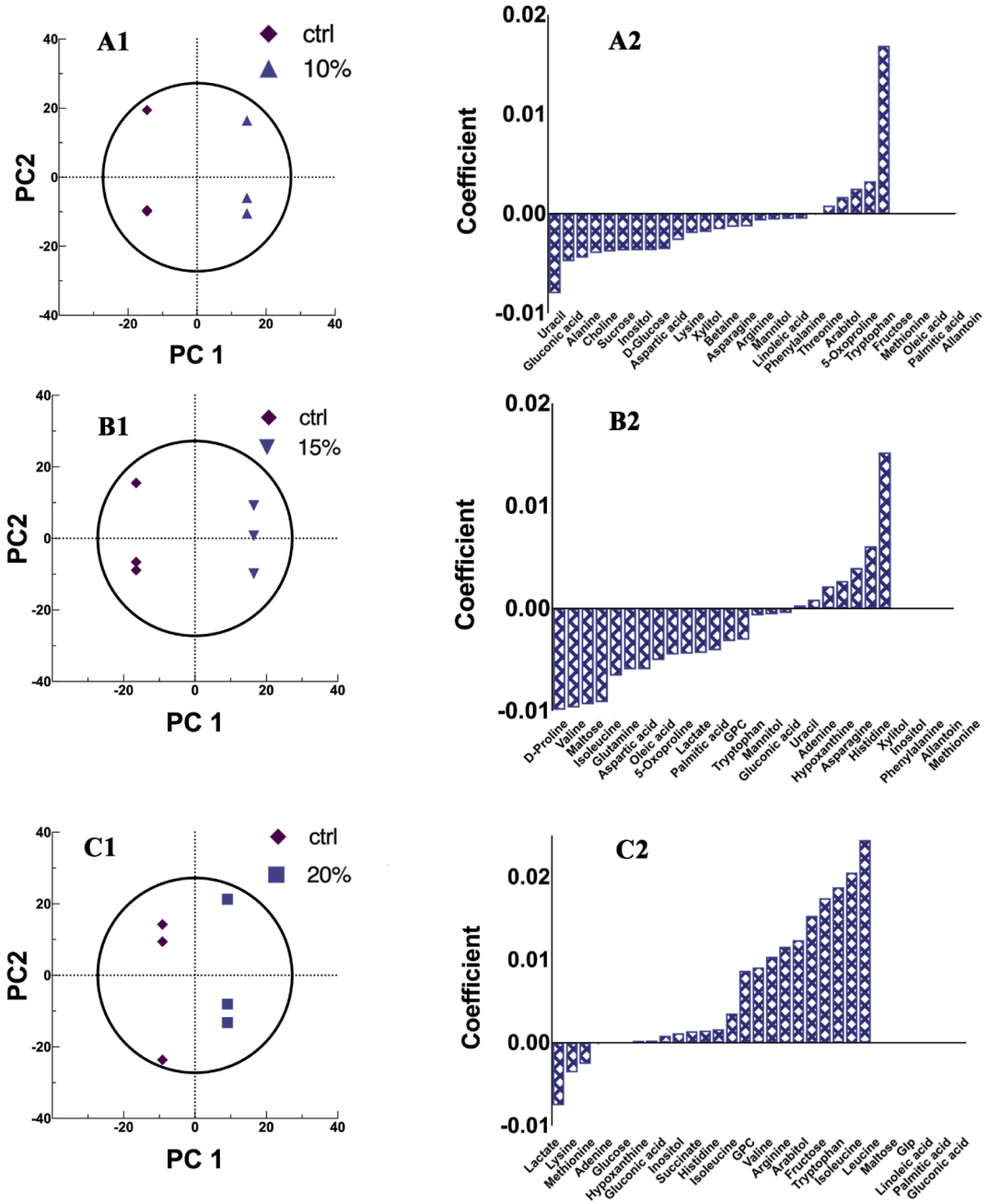

Fig. 3. Orthogonal projection to latent structures-discriminant analysis (OPLS-DA) between control and treatment groups. A1-A2: Score plot and coefficient plot of control and WKN 10; B1-CB2: Score plot and coefficient plot of control and WKN 15; C1-C2: Score plot and coefficient plot of control and WKN 20. Note: WKN 10, WKN 15 and WKN20 represent noodle at 10%, 15% and 20% wakame replacement, respectively.

including Aminoacyl-tRNA biosynthesis, valine, leucine and isoleucine biosynthesis, alanine, aspartate and glutamate metabolism, galactose metabolism, arginine biosynthesis, starch and sucrose metabolism, pantothenate and CoA biosynthesis, beta-Alanine metabolism, glycine, serine and threonine metabolism, glycerophospholipid metabolism, biosynthesis of unsaturated fatty acids, neomycin, kanamycin and gentamicin biosynthesis and histidine metabolism. Forty-six pathways were involved and eleven of metabolic pathways were significantly affected on the WKN 15 sample through *in vitro* digestion, including Aminoacyl-tRNA biosynthesis, Val, Leu and Ile biosynthesis, Ala, Asp and Glu metabolism, Arg biosynthesis, Starch and sucrose metabolism, Galactose metabolism, Gly, Ser and Thr metabolism, Glycerophospholipid metabolism, Biosynthesis of unsaturated fatty acids and His metabolism.

Since there were several components of proteins (e.g., peptides, lectins, amino acids, and glycoproteins) which were highly contained by wakame, the nutritional value of WKN depends on the quantity and quality of metabolites, such as amino acid composition, ratios of pathways, propensity to hydrolysis during digestion. To illustrate the alternations visually and clearly, a schematic of significant pathways and metabolites *in vitro* is shown in Fig. 6, where the color of blocks revealed the changes of metabolite content: the bluish and greenish ones showed the low and high metabolite level, respectively; the color of arrows represented the changes of pathway classes. The major metabolisms were divided into amino acid, carbohydrate, and fatty acid pathway.

For the amino acid metabolism, the concentrations of leucine, isoleucine and valine released from WKN sample were increased with the addition of wakame compared with control group. This observation

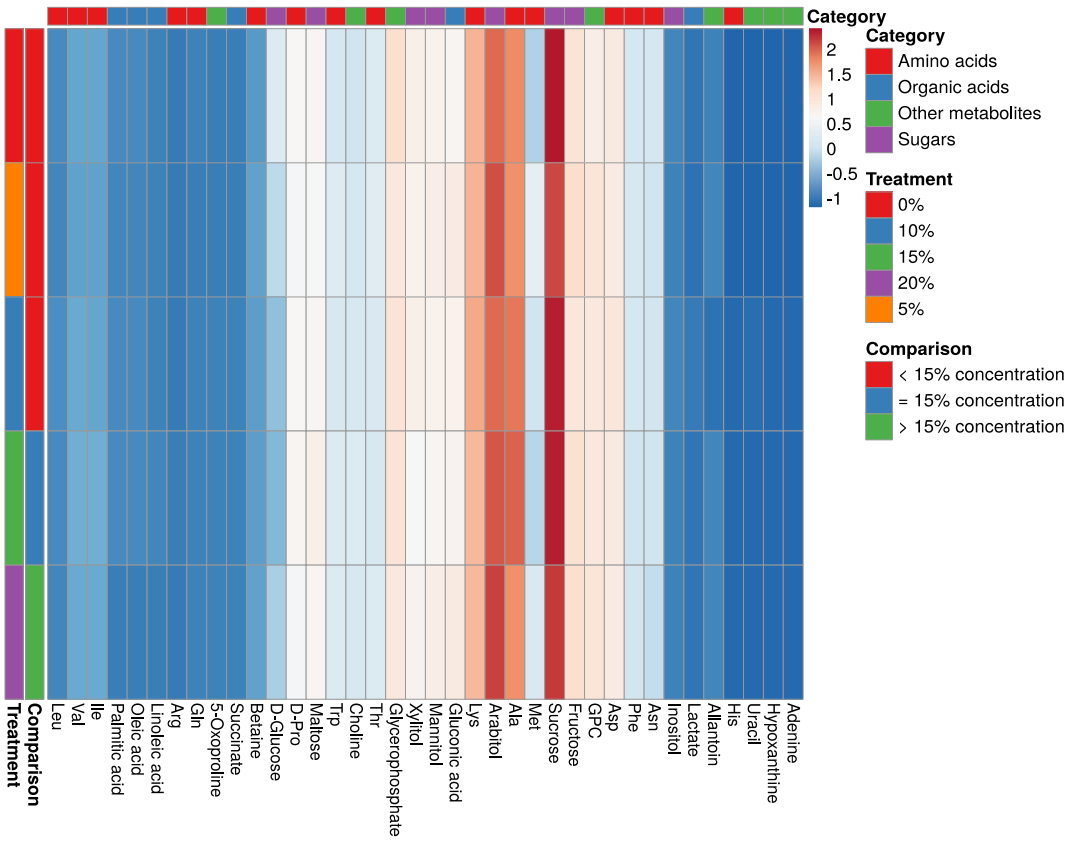

Fig. 4. Heatmap of identified metabolites of noodles after *in vitro* digestion. Note: 0%, 5%, 10%, 15%, and 20% represents noodle at 0%, 5%, 10%, 15% and 20% wakame powder replacement, respectively.

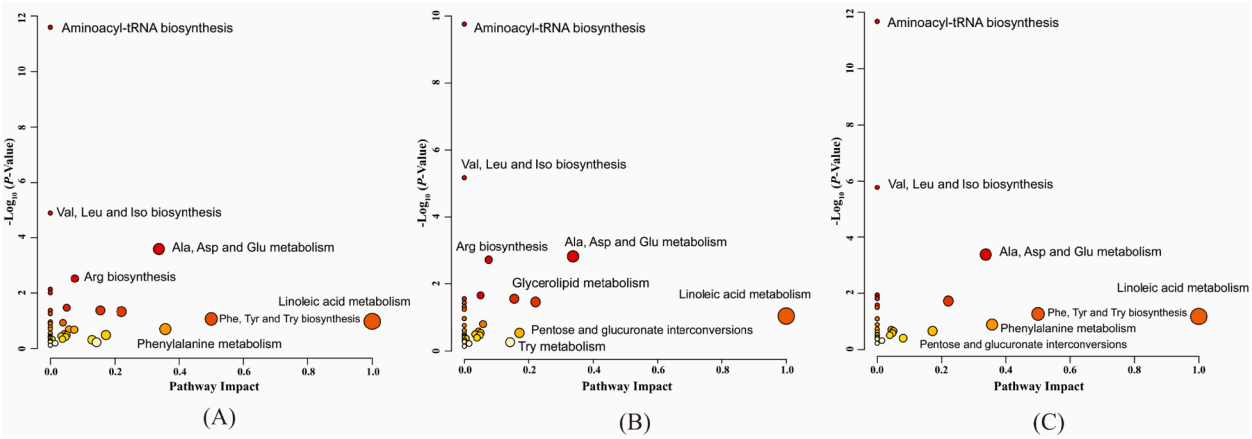

Fig. 5. Metabolic pathways altered in control and WKN 10 (A); control and WKN 15 (B); control and WKN 20 (C). Note: WKN 10, WKN 15 and WKN 20 represents wakame noodles at 10%, 15%, and 20% wakame powder replacement, respectively.

indicated that protein may be hydrolyzed with digestive enzymes into peptides and finally broken down into amino acids, revealing that wakame has greatly increased the absorption of proteins. Glucose-6-Phosphate (G6P) was converted to pyruvate and coupled with reduced nicotinamide adenine dinucleotide (NADH) generation (Wei, Quarterman, & Jin, 2013; Xia, Jacob, Herrmann, Tabassum, & Murphy, 2015). Alanine, aspartic acid, glycerophosphate, and threonine were usually produced via consuming pyruvate. The production pathways of phenylalanine, tyrosine, tryptophan and consumed acetoacetyl CoA. The production pathways of isoleucine, valine and leucine showed positive effects for amino acid production using acetyl CoA.

As for carbohydrate metabolism, starch is partially broken down into maltose, glucose, and fructose by an α-amylase enzyme step in the oral cavity (Woolnough, Bird, Monro, & Brennan, 2010). The rates of monosaccharides in this digesta was very high. WKN digesta consists primarily of rhamnose, xylose, fucose, alginate, mannitol and laminarin at high concentrations while glucose is limited in quantity (Zhang, Yuen, de Nys, Masters, & Maschmeyer, 2020). It can be explained by fucoidan (25–30% of the wakame (Ngo, Wijesekara, Vo, Van Ta, & Kim, 2011)), a polysaccharide usually composed of L-Fucose units connected by (1–4) and (1–3) glycosidic bonds containing sulfation at position 2, 3, and/or 4. In combination with other polysaccharides such as xylose and mannitol, it can form more complex chain structures. (Gómez-Ordóñez & Rupérez, 2011; Kang, et al., 2008; Rodriguez-Jasso, Mussatto,

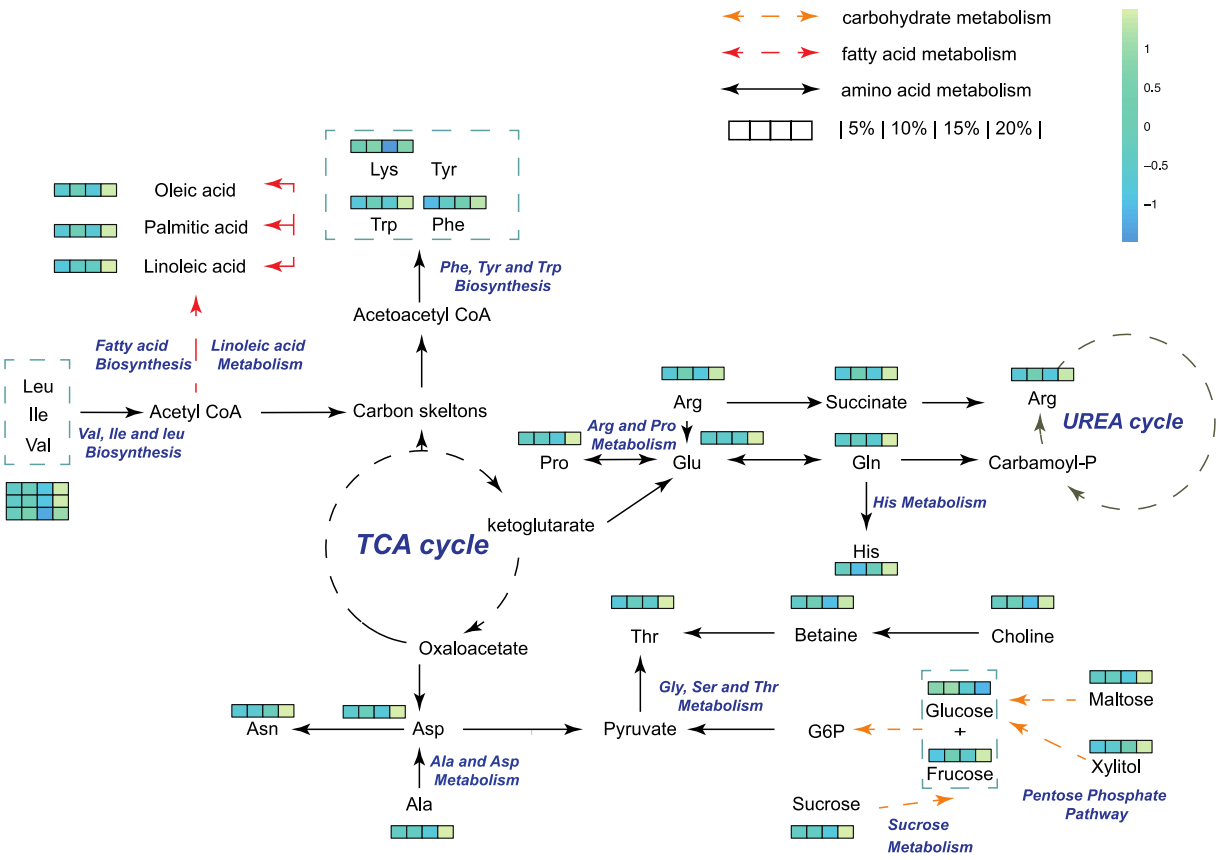

Fig. 6. Proposed schematic of metabolic alterations of wakame noodle. Note: 5%, 10%, 15%, and 20% represents wakame noodles at 5%, 10%, 15% and 20% wakame powder replacement, respectively.

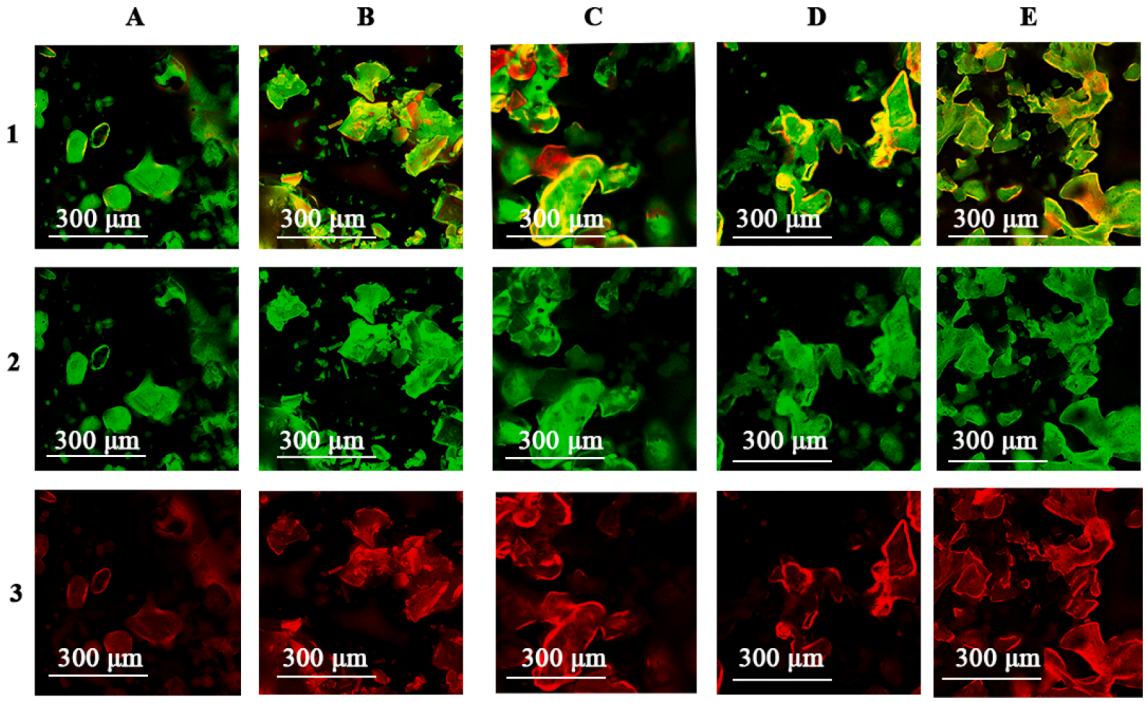

Fig. 7. Microstructure of the wakame noodles prepared with wakame at 0% (A1; A2;A3), 5% (B1; B2; B3), 10% (C1; C2; C3), 15% (D1; D2; D3), 20% (E1; E2; E3). Note: 0%, 5%, 10%, 15%, and 20% represents noodle at 0%, 5%, 10%, 15% and 20% wakame powder replacement, respectively. *Figures labelled with 1 were overlay channel; while those labelled with 2 were from fluorescein isothiocyanate (FITC) channel and those labelled with 3 were from Nile Red channel. (For interpretation of the references to color in this figure legend, the reader is referred to the web version of this article.)

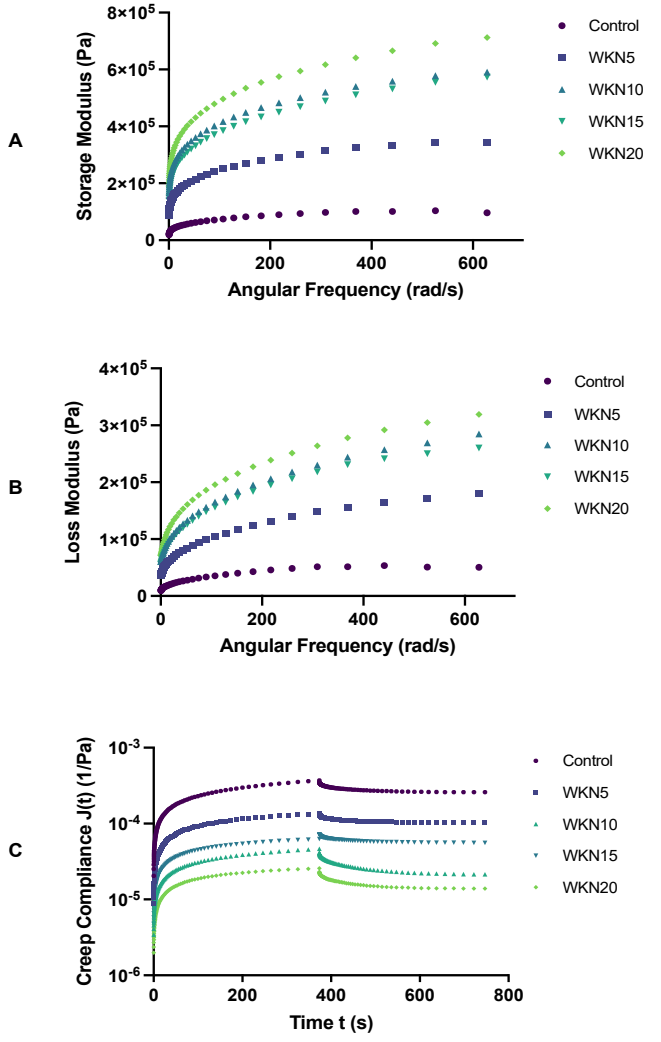

Fig. 8. The storage modulus (A), loss modulus (B) and creep compliance (C) of control noodle and wakame noodles. Note: WKN 5, WKN 10, WKN 15 and WKN20 represents noodle at 5%, 10%, 15% and 20% wakame powder replacement, respectively.

Table 2
Power-Law model of the wakame noodles prepared with wakame at 0% (raw dough; noodle digesta), 5% (raw dough; noodle digesta), 10% (raw dough; noodle digesta), 15% (raw dough; noodle digesta), 20% (raw dough; noodle digesta).

Power-law	K_f (kPa·s^n)	R^2	RMSE	SSR
Raw dough				
0%	2.53 ± 0.10^d	0.99	0.016	0.010
5%	10.58 ± 1.10^c	0.99	0.010	0.003
10%	18.73 ± 3.03^{ab}	0.99	0.006	0.002
15%	16.70 ± 1.50^b	0.99	0.008	0.002
20%	22.60 ± 4.10^a	0.99	0.010	0.004
Noodle digesta				
	K_f (Pa·s^n)	R^2	RMSE	SSR
0%	0.05 ± 0.01	0.98	0.092	0.169
5%	0.14 ± 0.09	0.99	0.027	0.015
10%	0.07 ± 0.04	0.99	0.041	0.033
15%	0.06 ± 0.01	0.99	0.101	0.203
20%	0.13 ± 0.01	0.99	0.122	0.299

Different superscript letters in rows are significantly different using one-way ANOVA and Duncan's multiple range test ($P < 0.05$). Each point corresponds to the average value ± standard deviation.

Table 3
Burger model of the wakame noodles prepared with wakame at 0% (creep phase; recovery phase), 5% (creep phase; recovery phase), 10% (creep phase; recovery phase), 15% (creep phase; recovery phase), 20% (creep phase; recovery phase).

	r_1(s)	r_2 (s)	r_3 (s)	R^2	RMSE (10^{-6})	SSR (10^{-9})
Creep phase						
0%	59.78 ± 4.16	5.85 ± 0.04	0.47 ± 0.05	0.99	38.69	1.197
5%	55.95 ± 7.59	5.35 ± 0.23	0.44 ± 0.02	0.99	8.673	6.017
10%	58.91 ± 6.79	5.80 ± 0.94	0.51 ± 0.10	0.99	4.956	1.965
15%	51.39 ± 1.32	5.84 ± 0.37	0.48 ± 0.04	0.99	1.700	0.231
20%	53.96 ± 5.76	5.74 ± 1.11	0.47 ± 0.14	0.99	2.834	0.643
Recovery phase						
0%	90.43 ± 11.10	10.79 ± 0.86	0.90 ± 0.15	0.99	4.649	1.729
5%	97.80 ± 37.13	11.93 ± 5.22	0.86 ± 0.17	0.99	3.982	1.269
10%	93.82 ± 10.18	11.10 ± 3.03	0.94 ± 0.26	0.99	9.680	7.496
15%	78.71 ± 5.93	8.99 ± 0.88	0.73 ± 0.05	0.99	0.786	4.937
20%	77.01 ± 6.36	9.29 ± 1.64	0.75 ± 0.15	0.99	0.425	1.441

Pastrana, Aguilar, & Teixeira, 2011).

Since NMR analysis may overvalue the glucose due to the unseparated spectra, the glucose content after *in vitro* digestion was tested via GO assay kit. With the wakame addition, the glucose level after *in vitro* digestion represented a lower trend, which matched well with Huang, et al. (2021). It may be since bioactive peptides from wakame proteins have established effect in regulating glucose homeostasis. The glucose level of the WKN 20 was decreased by 23.3% compared to WKN 5, which could be ascribed to a relative resistant effect through digestion by high dietary fiber content in the wakame. To be specific, dietary fiber contributed to the viscous substance of digestive system so that they inhibited the absorption of glucose by shielding sugar through the intestines (Opazo-Navarrete, et al., 2018).

After *in vitro* digestion, high dietary fiber content may cause a low glycaemia response, which plays a crucial role in diabetes. Wheat flour noodles that are rich in starch would lead to a dramatically increase of the risk for diabetes due to the increasing postprandial glycemic responses, recent research has highlighted the utilization of wakame which is rich in antidiabetic peptides for the management of type 2 diabetes (Pimentel, Alves, Harnedy, FitzGerald, & Oliveira, 2019). Despite this work discovering anti-diabetes function was limited, it still showed a promising prospective of WKN as potential nutraceutical. After stimulated oral digestion, incomplete digested starch produced short-chain fatty acids by pancreatin action (Dona, Pages, Gilbert, & Kuchel, 2010).

According to our hypothesis, WKN would reduce cholesterol concentrations since it increases choline concentrations with the increasing wakame addition to the noodles, thereby reducing cholesterol absorption during intestinal digestion. This observation matched well with previous work, suggesting fucoxanthin and dietary fiber are part of wakame, which may decrease concentration of cholesterol (Oliyaei, Moosavi-Nasab, Tamaddon, & Fazaeli, 2020). Hence, oleic acid, palmitic acid, and linoleic acid concentrations are influenced by the small intestine digestion of lipid and/or biosynthesis of fatty acids (Ravi & Baskaran, 2015). Present study supports the hypothesis that the yield of fatty acid synthesis and oxidation has been associated with the wakame diets (Kirke, Smyth, Rai, Kenny, & Stengel, 2017).

In the present study, reciprocal responses in acetyl-CoA, which is the

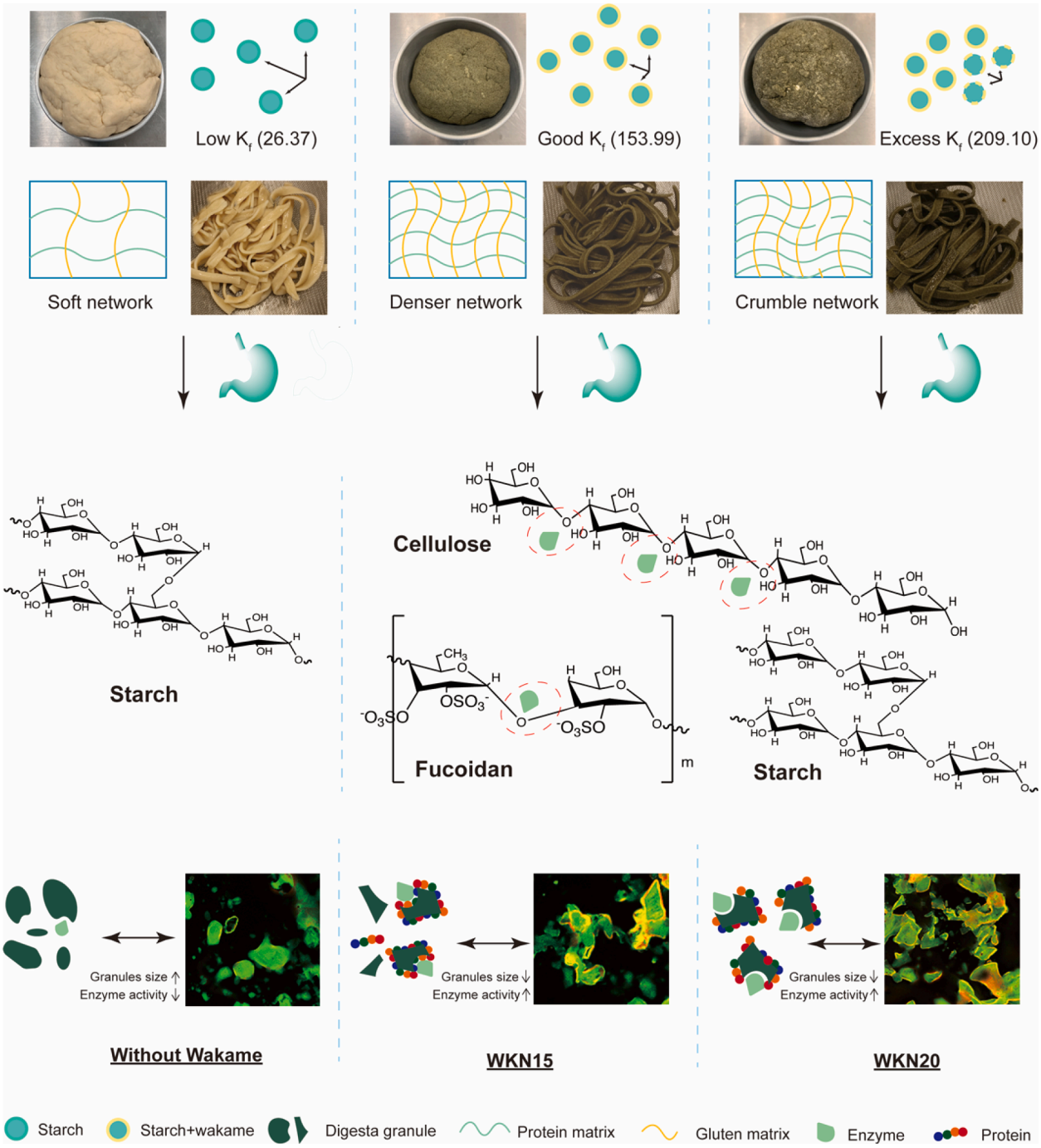

Fig. 9. The proposed schematic model illuminating the physicochemical properties of wakame noodle (WKN) on the *in vitro* digestion. Notes: WKN 15 and WKN20 represents noodle at 15% and 20% wakame addition, respectively.

enzyme of fatty acid synthesis were also observed in having effects on Val, Ile, and Leu biosynthesis with wakame diets and the control diet. Therefore, the extent of increased activities of acetyl-CoA further proved that probably wakame addition accumulated the fatty acid metabolisms and cholesterol-lowing effects. Due to the increased ratio of linoleic acid to total fatty acids, wakame diets significantly altered fatty acid biosynthesis, suggesting that there appears to be an increase in the activity of linoleic acid as a substrate reacting with glycolipid biosynthesis enzymes as well as enzymes for fatty acid desaturation and chain lengthening (Fernandez-Segovia, Lerma-Garcia, Fuentes, & Barat, 2018).

Overall, enriching wheat noodle with the ingredient obtained from the wakame allows for the supplementation of noodle with compounds (proteins, dietary fibers, fucoxanthin, and fatty acids) that have had their antioxidant and pro-health properties thoroughly documented (Fung, et al., 2013; H. D. Wang, Li, Lee, & Chang, 2017).

3.7. *Confocal laser scanning microscopy (CLSM)*

From the Fig. 7, CLSM was used to observe and illustrate the influence of proteins in the noodle samples. As for the color change, compared to the control group, the yellow color around the aggregation has obviously colored, indicated that the proteins of WKN which distributed around the edge of the starch. This revealed that the wakame

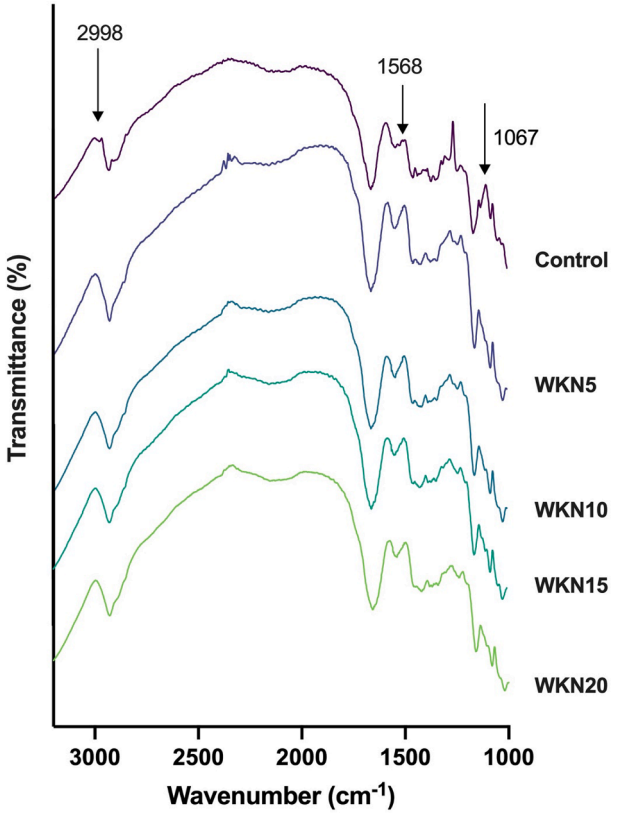

Fig. 10. FTIR spectra for noodles containing wheat starch and wakame. The lines from top to bottom represents control group, WKN5, WKN10, WKN15, and WKN20 respectively. Note: WKN 5, WKN 10, WKN 15 and WKN20 represents noodle at 5%, 10%, 15% and 20% wakame powder replacement, respectively.

protein contributed to the connection of the green starch granules. This was also supported by the thin film of protein network, which seems to be formed and gelatinized entirely to enclose starch granules. As for the structural characterization, compared to the control group, the morphology changed considerably on WKN digesta, especially on WKN 5 and WKN 20 groups. The aggregation was changed from irregular ellipses to smaller angular diamonds, indicated that, in agreement with a previous study (Lu, Ma, Qiu, Sun, & Tian, 2021). The effect of wakame proteins on *in vitro* digestion appeared to the minimizing of granules size, which may increase the joint sites for digestive enzymes (Liu, Yang, Guo, Xing, & Zhu, 2021). In addition, these observations successfully proved our metabolite analysis.

3.8. Rheology features

To evaluate the mechanical specification of noodle dough in the presence and lack of wakame at different concentrations, the frequency sweep was tested out (Fig. 8) and power law model fitting results are shown in Table 2. Gluten cross-linking strength is known to have a significant impact on the rheological properties of dough and noodles. Although the dietary fiber contained in wakame also facilitates the absorption of water, thereby preventing the cross-linking of gluten proteins (Liang, et al., 2020), the viscoelastic curves rose significantly. It can also be observed by a higher K_f when its cross-linking strength is greater. When the substitution amount was 20%, K_f reached a maximum. This could be explained because of interactions between proteins and fibers in the fabric, a more stable network structure is formed.

As the wakame contained plenty of fibers, water rapidly absorbed and influences the cross-bonding of gluten protein (Liang, et al., 2020). As a result of 15% wakame being added to wheat flour, wheat gluten proteins were diluted and the network structure of wheat gluten was broken, thus decreasing the viscoelasticity of dough. A significant influence on the rheological properties of dough or noodles can be attributed to the cross-linking strength of gluten. As gluten has a higher cross-linking strength, its K_f is always higher in WKN dough. Alternatively, the curves of viscoelasticity rose under other conditions. Approximately 20% substitution resulted in the maximum value of K_f. A more stable network structure could be explained by the proteins and fibers in the dough interacting appropriately with one another (Iqbal, Wu, Kirk, & Chen, 2021). Moreover, the viscoelasticity was increased as increasing polymeric proteins (Zhang, Chen, Qi, Sui, & Jiang, 2018). In general, the wakame flour formed a good cross-linking network structure and had better viscosity than the control, the elasticity of dough reached our expectation (Zhang, Ma, Yang, Li, & Sun, 2022).

Table 3 shows the Burger model results of boiled WKN and control noodles. In the creep phase, wakame flour concentration clearly influences the creep curves which is also reflected in the model parameters. Steady state viscosity μ_0 increases and reaches a constant value at the addition between WKN10 to WKN15 and then increases significantly at the addition of WKN20. Increasing μ_0 induces the higher dough viscosity which can be used to support the effects between viscosity and metabolism. For the recovery phase, no significant changes in retardation times values (r_1, r_2, and r_3) but the steady state viscosity μ_0 showed a decrease with increasing wakame addition. It seems that wakame addition does not affect the speed of the recovery since stable retardation times, indicating a consistent retarded elastic response. The plateau in total recovery between control to WKN15 is also seen in the model parameters as J_1, J_2, and J_3 stay relatively constant. For the r_1, r_2, and r_3, a significant decrease is observed with increasing composition of wakame flour more than WKN15. This means that retarded elastic recovery takes place faster when the sample is composed of high level of wakame.

3.9. Schematic model

From all these results, a schematic diagram was proposed (Fig. 9) based on the physiochemical properties-interaction-structure relationship and metabolic changes.

Before *in vitro* digestion, the gelatinization of WKN15 and WKN20 was significantly higher than that of control noodles, suggesting that the higher amount of wakame led to an increased ability to gelatinize with the gluten matrix, thus increasing the apparent viscosity. In addition, the viscosity of WKN20 was significantly increased compared to WKN15, which may since the stable complex formed by the protein matrix and gluten matrix was again broken and could not encapsulate the whole gelatinized starch granules, thus may affect the subsequent cooking quality.

After *in vitro* digestion, the addition of wakame not only increased the amino acid and fatty acid content compared to control noodle, but also formed a significant amount of fucoidan and cellulose, which may help maintain body weight and postprandial blood glucose levels. Along with the different interactions discussed above, the homogeneous distribution of green and yellow areas observed under CLSM supports the WKN (noodle contains wakame) surface formed a thin protein network and the granules changed from an ellipse-like shape to a smaller diamond-like shape.

Thus, the associations of wakame to improve the nutritional value of noodles could be interpreted in different ways. Firstly, the wakame-induced increased the breakdown of digesta particles was a reason of the higher amino acids' concentration. Smaller particles are typically more contribute to enzymatic digestion than larger particles due to the increasing joint sites for enzyme. Secondly, the presence of the protein network impairs the contact of starch molecules with amylolytic enzymes due to the increase in viscosity and envelope barriers, which is an effective way with low glycemic load and high satiety (Liu et al., 2018).

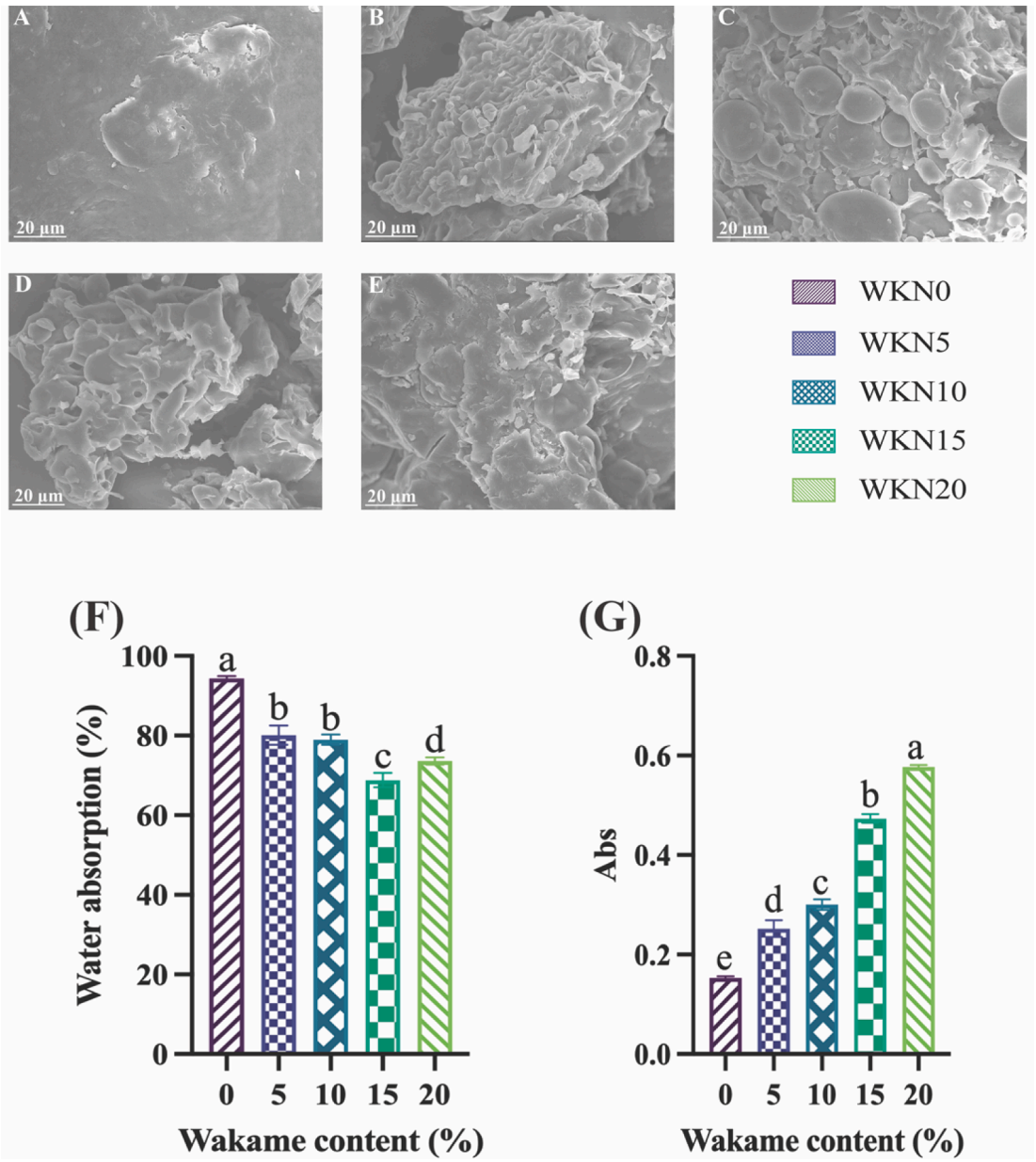

Fig. 11. SEM micrographs of the wakame noodles prepared with wakame at 0% (A), 5% (B), 10% (C), 15% (D), 20% (E), water absorption (F) and turbidity (G).

3.10. Validation via FT-IR spectroscopy

The FTIR of WKN was processed to analyze the secondary structure. Six peaks that were typical absorption peaks of starch at the wavenumbers of 1067 to 2996 cm^{-1} are shown in Fig. 10. It showed that there was no new characteristic peak after adding wakame to the starch-based noodles. Among them, the peak at 2996 cm^{-1} represented stretching vibration peak of the hydroxyl group, the peak at 1568 cm^{-1} represented the stretching vibration of C=O, which indicated beta-sheet structure of proteins and were mainly generated by serine (Rafiquzzaman et al., 2015). The other two peaks at 1067 cm^{-1} represented the stretching vibration of C-O and bending vibration of C-OH in starch (Xu et al., 2022). Moreover, with the increase of wakame level, hydrogen bond interactions formed between wakame, and starch contributed to the general shift of lower band at 1067 cm^{-1} (Han, Ma, Yang, Li, & Sun, 2021; Xu et al., 2022). The fact that peak positions and fundamental bands did not differ significantly among groups suggests that different amounts of hydrocolloids may not significantly alter the hydroxyl groups of the noodles (Lu, Lee, & Yang, 2022). All the spectra are similar in shape and bands' position and orientation regardless of the wakame added.

3.11. Validation via SEM

From the Fig. 11, the SEM images of WKN with different concentrations after cooking displayed network-structures as expected. It could be clearly seen from Fig. 9C that the network was tighter from WKN 5 to WKN 10 regardless of heartland or fringe part. This continuous network might be formed with gluten matrix and protein matrix of WKN samples as the higher amount of wakame leading to increasing gumming ability with gluten matrix, which further supported the conclusion of TPA. For WKN 10 and WKN 15, protein formed a stable complex with starch, which could give cooked noodles a beneficial effect on texture characteristics since it had low cooking loss (Liu, Song, Tao, Yu, & Wang, 2022). When the WKN content was 15% and 20%, respectively, it was found with the higher specific volume and porosity, in consensus with our CLSM analysis, leading to more approachability of enzyme to proteins and starch granules, which became more easily taken in

hydrolysing as mentioned above (Lau, Soong, Zhou, & Henry, 2015). Similarly, previous studies revealed the enhanced interaction between starch granules and protein matrix in pasta containing seaweeds up to 20% (Prabhasankar, et al., 2009). Hence, when concentration of wakame beyond 20% was used, network seems showed trend to collapse again, which could be explained that excess wakame (>20%) would weaken the compound-remaining ability of network due to a higher cooking loss (Han, Ma, Li, & Sun, 2020; Prabhasankar, et al., 2009).

4. Conclusion

2D ^{1}H–^{13}C NMR spectroscopy, principal component analysis (PCA), and orthogonal projections to latent structures-discriminant analysis (OPLS-DA) were used for authentication of metabolite compounds released in the conditions parallel to those in the human digestive tract. It can be concluded that metabolite fingerprinting using ^{1}H–^{13}C NMR spectroscopy provides a great tool for authentication. The texture analyses, rheological measurements, SEM and FTIR, etc. were used to explore extruded wakame flours improve the texture and viscoelasticity of noodle qualities. Extruded wakame flour with dynamic viscosity functioned as adhesives, which can hold starch granules and other components within flours together, as indicated from several mathematic models. Wakame can be added to wheat flour at 5%–15%, depending on the preference of texture quality for the type of noodles. The use of brown seaweed in various starch food systems may be supported by this study in view of wakame's reputation as a healthy food ingredient.

Uncited references

CRediT authorship contribution statement

Yi Kai: Conceptualization, Methodology, Investigation, Software, Visualization, Validation, Writing – original draft, Writing – review & editing. **Yi Liu:** Methodology. **Hongliang Li:** Methodology. **Hongshun Yang:** Conceptualization, Funding acquisition, Project administration, Supervision, Writing – review & editing.

Declaration of Competing Interest

The authors declare that they have no known competing financial interests or personal relationships that could have appeared to influence the work reported in this paper.

Data availability

The data that has been used is confidential.

Acknowledgements

This study was funded by Singapore Ministry of Education Academic Research Fund Tier 1 (A-8000469-00-00) and an industry project supported by Guangzhou Welbon Biological Co., Ltd (A-0008525-00-00).

Appendix A. Supplementary data

Supplementary data to this article can be found online at https://doi.org/10.1016/j.foodres.2022.112394.

References

Cao, Z.-B., Yu, C., Yang, Z., Xing, J.-J., Guo, X.-N., & Zhu, K.-X. (2021). Impact of gluten quality on textural stability of cooked noodles and the underlying mechanism. *Food Hydrocolloids, 119*, Article 106842.

Chen, L., Liu, Q., Zhao, X., Zhang, H., Pang, X., & Yang, H. (2022). Inactivation efficacies of lactic acid and mild heat treatments against *Escherichia coli* strains in organic broccoli sprouts. *Food Control, 133*, Article 108577.

Cho, Y., Kim, H., & Kim, S. K. (2013). Bioethanol production from brown seaweed, *Undaria pinnatifida*, using NaCl acclimated yeast. *Bioprocess and Biosystems Engineering, 36*(6), 713–719.

Dona, A. C., Pages, G., Gilbert, R. G., & Kuchel, P. W. (2010). Digestion of starch: *In vivo* and *in vitro* kinetic models used to characterise oligosaccharide or glucose release. *Carbohydrate Polymers, 80*(3), 599–617.

Fabek, H., Messerschmidt, S., Brulport, V., & Goff, H. D. (2014). The effect of *in vitro* digestive processes on the viscosity of dietary fibres and their influence on glucose diffusion. *Food Hydrocolloids, 35*, 718–726.

Fernandez-Segovia, I., Lerma-Garcia, M. J., Fuentes, A., & Barat, J. M. (2018). Characterization of Spanish powdered seaweeds: Composition, antioxidant capacity and technological properties. *Food Research International, 111*, 212–219.

Fitzgerald, C., Mora-Soler, L., Gallagher, E., O'Connor, P., Prieto, J., Soler-Vila, A., & Hayes, M. (2012). Isolation and characterization of bioactive pro-peptides with *in vitro* renin inhibitory activities from the macroalga *Palmaria palmata*. *Journal of Agricultural and Food Chemistry, 60*(30), 7421–7427.

Fung, A., Hamid, N., & Lu, J. (2013). Fucoxanthin content and antioxidant properties of *Undaria pinnatifida*. *Food Chemistry, 136*(2), 1055–1062.

Gasparre, N., & Rosell, C. M. (2019). Role of hydrocolloids in gluten free noodles made with tiger nut flour as non-conventional powder. *Food Hydrocolloids, 97*.

Gómez-Ordóñez, E., & Rupérez, P. (2011). FTIR-ATR spectroscopy as a tool for polysaccharide identification in edible brown and red seaweeds. *Food Hydrocolloids, 25*(6), 1514–1520.

Guo, X. N., Wei, X. M., & Zhu, K. X. (2017). The impact of protein cross-linking induced by alkali on the quality of buckwheat noodles. *Food Chemistry, 221*, 1178–1185.

Han, C., Ma, M., Li, M., & Sun, Q. (2020). Further interpretation of the underlying causes of the strengthening effect of alkali on gluten and noodle quality: Studies on gluten, gliadin, and glutenin. *Food Hydrocolloids, 103*, Article 105661.

Han, C., Ma, M., Yang, T., Li, M., & Sun, Q. (2021). Heat mediated physicochemical and structural changes of wheat gluten in the presence of salt and alkali. *Food Hydrocolloids, 120*, 106971.

Huang, M., Zhao, X., Mao, Y., Chen, L., & Yang, H. (2021). Metabolite release and rheological properties of sponge cake after *in vitro* digestion and the influence of a flour replacer rich in dietary fibre. *Food Research International, 144*, Article 110355.

Iqbal, S., Wu, P., Kirk, T. V., & Chen, X. D. (2021). Amylose content modulates maize starch hydrolysis, rheology, and microstructure during simulated gastrointestinal digestion. *Food Hydrocolloids, 110*, Article 106171.

Kang, K. S., Kim, I. D., Kwon, R. H., & Ha, B. J. (2008). *Undaria pinnatifida* fucoidan extract protects against CCl4-induced oxidative stress. *Biotechnology and Bioprocess Engineering, 13*(2), 168–173.

Khatkar, B. S., Barak, S., & Mudgil, D. (2013). Effects of gliadin addition on the rheological, microscopic and thermal characteristics of wheat gluten. *International Journal of Biological Macromolecules, 53*, 38–41.

Kim, H., Ra, C. H., & Kim, S.-K. (2013). Ethanol production from seaweed (*Undaria pinnatifida*) using yeast acclimated to specific sugars. *Biotechnology and Bioprocess Engineering, 18*(3), 533–537.

Kirke, D. A., Smyth, T. J., Rai, D. K., Kenny, O., & Stengel, D. B. (2017). The chemical and antioxidant stability of isolated low molecular weight phlorotannins. *Food Chemistry, 221*, 1104–1112.

Lau, E., Soong, Y. Y., Zhou, W., & Henry, J. (2015). Can bread processing conditions alter glycaemic response? *Food Chemistry, 173*, 250–256.

Liu, F. Y., Yang, Z., Guo, X. N., Xing, J. J., & Zhu, K. X. (2021). Influence of protein. type, content and polymerization on in vitro starch digestibility of sorghum noodles. *Food Research International, 142*, Article 110199.

Li, M., Dhital, S., & Wei, Y. (2017). Multilevel structure of wheat starch and its relationship to noodle eating qualities. *Comprehensive Reviews in Food Science and Food Safety, 16*(5), 1042–1055.

Liang, X., Ma, C., Yan, X., Zeng, H., McClements, D. J., Liu, X., & Liu, F. (2020). Structure, rheology and functionality of whey protein emulsion gels: Effects of double cross-linking with transglutaminase and calcium ions. *Food Hydrocolloids, 102*, Article 105569.

Liu, D., Song, S., Tao, L., Yu, L., & Wang, J. (2022). Effects of common buckwheat bran on wheat dough properties and noodle quality compared with common buckwheat hull. *LWT-Food Science and Techology, 155*, Article 112971.

Liu, L., Yang, W., Cui, S. W., Jiang, Z., Chen, Q., Qian, H., … Zhou, S. (2018). Effects of pentosanase and glucose oxidase on the composition, rheology and microstructure of whole wheat dough. *Food Hydrocolloids, 84*, 545–551.

Lu, X., Ma, R., Qiu, H., Sun, C., & Tian, Y. (2021). Mechanism of effect of endogenous/exogenous rice protein and its hydrolysates on rice starch digestibility. *International Journal of Biological Macromolecules, 193*(Pt A), 311–318.

Lu, Z., Lee, P. R., & Yang, H. (2022). Chickpea flour and soy protein isolate interacted with κ-carrageenan via electrostatic interactions to form egg omelets analogue. *Food Hydrocolloids, 130*, 107691.

Lucas-Gonzalez, R., Viuda-Martos, M., Perez-Alvarez, J. A., & Fernandez-Lopez, J. (2018). In vitro digestion models suitable for foods: Opportunities for new fields of application and challenges. *Food Research International, 107*, 423–436.

Ma, M., Xu, Z., Chen, X., Zhang, C., Liu, Z., Cantre, D., … Corke, H. (2022). Architecture of outer shell and inner blocklets of rice starch granule is related to starch granule-associated proteins. *Food Hydrocolloids, 127*, Article 107551.

Mudgil, D., Barak, S., & Khatkar, B. S. (2016). Effect of partially hydrolyzed guar gum on pasting, thermo-mechanical and rheological properties of wheat dough. *International Journal of Biological Macromolecules, 93*(Pt A), 131–135.

Nadeeshani, H., Hassouna, A., & Lu, J. (2021). Proteins extracted from seaweed *Undaria pinnatifida* and their potential uses as foods and nutraceuticals. *Critical Reviews in Food Science and Nutrition*, 1–17.

Nawaz, A., Xiong, Z., Xiong, H., Chen, L., Wang, P. k., Ahmad, I., Hu, C., Irshad, S., & Ali, S. W. (2018). The effects of fish meat and fish bone addition on nutritional value, texture and microstructure of optimised fried snacks. *International Journal of Food Science & Technology, 54*(4), 1045-1053.

Ngo, D.-H., Wijesekara, I., Vo, T.-S., Van Ta, Q., & Kim, S.-K. (2011). Marine food-derived functional ingredients as potential antioxidants in the food industry: An overview. *Food Research International, 44*(2), 523–529.

Oliyaei, N., Moosavi-Nasab, M., Tamaddon, A. M., & Fazaeli, M. (2020). Encapsulation of fucoxanthin in binary matrices of porous starch and halloysite. *Food Hydrocolloids, 100*, Article 105458.

Ojukwu, M., Tan, J. S., & Easa, A. M. (2020). Cooking, textural, and mechanical properties of rice flour-soy protein isolate noodles prepared using combined treatments of microbial transglutaminase and gluconolactone. *Journal of food science, 85*(9), 2720–2727.

Opazo-Navarrete, M., Tagle Freire, D., Boom, R. M., & Janssen, A. E. M. (2018). The influence of starch and fibre on *in vitro* protein digestibility of dry fractionated quinoa seed (riobamba variety). *Food Biophysics, 14*(1), 49–59.

Pimentel, F. B., Alves, R. C., Harnedy, P. A., FitzGerald, R. J., & Oliveira, M. B. P. (2019). Macroalgal-derived protein hydrolysates and bioactive peptides: Enzymatic release and potential health enhancing properties. *Trends in Food Science & Technology, 93*, 106–124.

Prabhasankar, P., Ganesan, P., Bhaskar, N., Hirose, A., Stephen, N., Gowda, L. R., … Miyashita, K. (2009). Edible Japanese seaweed, wakame (*Undaria pinnatifida*) as an ingredient in pasta: Chemical, functional and structural evaluation. *Food Chemistry, 115*(2), 501–508.

Rafiquzzaman, S. M., Kim, E. Y., Lee, J. M., Mohibbullah, M., Alam, M. B., Soo Moon, I., … Kong, I.-S. (2015). Anti-Alzheimers and anti-inflammatory activities of a glycoprotein purified from the edible brown alga *Undaria pinnatifida*. *Food Research International, 77*, 118–124.

Ran, X., Yang, Z., Chen, Y., & Yang, H. (2022). Konjac glucomannan decreases metabolite release of a plant-based fishball analogue during in vitro digestion by affecting amino acid and carbohydrate metabolic pathways. *Food Hydrocolloids, 129*, Article 107623.

Ravi, H., & Baskaran, V. (2015). Biodegradable chitosan-glycolipid hybrid nanogels: A novel approach to encapsulate fucoxanthin for improved stability and bioavailability. *Food Hydrocolloids, 43*, 717–725.

Rawiwan, P., Peng, Y., Paramayuda, I. G. P. B., & Quek, S. Y. (2022). Red seaweed: A promising alternative protein source for global food sustainability. *Trends in Food Science & Technology, 123*, 37–56.

Ribeiro, A. R., Madeira, T., Botelho, G., Martins, D., Ferreira, R. M., Silva, A. M. S., … Costa, R. (2022). Brown algae fucus vesiculosus in pasta: Effects on textural quality, cooking properties, and sensorial traits. *Foods, 11*(11), 1561.

Rioux, L.-E., Beaulieu, L., & Turgeon, S. L. (2017). Seaweeds: A traditional ingredients for new gastronomic sensation. *Food Hydrocolloids, 68*, 255–265.

Roberts, D. A., Paul, N. A., Dworjanyn, S. A., Bird, M. I., & de Nys, R. (2015). Biochar from commercially cultivated seaweed for soil amelioration. *Scientific Reports, 5*, 9665.

Rodriguez-Jasso, R. M., Mussatto, S. I., Pastrana, L., Aguilar, C. N., & Teixeira, J. A. (2011). Microwave-assisted extraction of sulfated polysaccharides (fucoidan) from brown seaweed. *Carbohydrate Polymers, 86*(3), 1137–1144.

Shao, L. F., Guo, X. N., Li, M., & Zhu, K. X. (2019). Effect of different mixing and kneading process on the quality characteristics of frozen cooked noodle. *LWT-Food Science and Techology, 101*, 583–589.

Wang, H. D., Li, X. C., Lee, D. J., & Chang, J. S. (2017). Potential biomedical applications of marine algae. *Bioresource Technology, 244*(Pt 2), 1407–1415.

Wang, L., Park, Y.-J., Jeon, Y.-J., & Ryu, B. (2018). Bioactivities of the edible brown seaweed, *Undaria pinnatifida*: A review. *Aquaculture, 495*, 873–880.

Wei, N., Quarterman, J., & Jin, Y. S. (2013). Marine macroalgae: An untapped resource for producing fuels and chemicals. *Trends in Biotechnology, 31*(2), 70–77.

Woolnough, J. W., Bird, A. R., Monro, J. A., & Brennan, C. S. (2010). The effect of a brief salivary alpha-amylase exposure during chewing on subsequent *in vitro* starch digestion curve profiles. *International Journal of Molecular Sciences, 11*(8), 2780–2790.

Xia, A., Jacob, A., Herrmann, C., Tabassum, M. R., & Murphy, J. D. (2015). Production of hydrogen, ethanol and volatile fatty acids from the seaweed carbohydrate mannitol. *Bioresource Technology, 193*, 488–497.

Xu, M., Hou, G. G., Ding, J., & Du, X. (2020). Comparative study on textural and rheological properties between dry white salted noodle and yellow alkaline noodle as influenced by different tea extracts. *Journal of Food Processing and Preservation, 44*(12), e14981.

Xu, X., Gao, C., Xu, J., Meng, L., Wang, Z., Yang, Y., … Tang, X. (2022). Hydration and plasticization effects of maltodextrin on the structure and cooking quality of extruded whole buckwheat noodles. *Food Chemistry, 374*, Article 131613.

Zhang, M., Ma, M., Yang, T., Li, M., & Sun, Q. (2022). Dynamic distribution and transition of gluten proteins during noodle processing. *Food Hydrocolloids, 123*.

Zhang, M., Zhang, L., Li, M., & Sun, Q. (2021). Inhibitory effects of sorbitol on the collapse and deterioration of gluten network in fresh noodles during storage. *Food Chemistry, 344*, Article 128638.

Zhang, R., Yuen, A. K. L., de Nys, R., Masters, A. F., & Maschmeyer, T. (2020). Step by step extraction of bio-actives from the brown seaweeds, *Carpophyllum flexuosum*, *Carpophyllum plumosum*, *Ecklonia radiata* and *Undaria pinnatifida*. *Algal Research, 52*, Article 102092.

Zhao, X., Chen, L., Wu, J., He, Y., & Yang, H. (2020). Elucidating antimicrobial mechanism of nisin and grape seed extract against *Listeria monocytogenes* in broth and on shrimp through NMR-based metabolomics approach. *International Journal of Food Microbiology, 319*, Article 108494.

Zhang, Y., Chen, S., Qi, B., Sui, X., & Jiang, L. (2018). Complexation of thermallydenatured soybean protein isolate with anthocyanins and its effect on the protein structure and in vitro digestibility. *Food Research International, 106*, 619–625.

Zhou, Y., Liu, J. J. H., Kang, Y., Cui, H., & Yang, H. (2021). Effects of acid and alkaline treatments on physicochemical and rheological properties of tilapia surimi prepared by pH shift method during cold storage. *Food Research International, 145*, Article 110424.

Zhu, J., Liu, Z., Chen, L., & Zheng, B. (2022). Impact of protein network restructured with soy protein and transglutaminase on the structural and functional characteristics of whole-grain highland barley noodle. *Food Hydrocolloids, 133*, Article 107909.